GDC-ASP-82-003

NASA-CR-167635

(NASA-CR-167635) SPACE CONSTRUCTION EXPERIMENT DEFINITION STUDY (SCEDS), PART 2. VOLUME 1: EXECUTIVE SUMMARY Final Report (General Dynamics/Convair) 32 p HC A03/MF A01 CSCL 22A G3/12 N82-29337 Unclas 28473

SPACE CONSTRUCTION EXPERIMENT DEFINITION STUDY (SCEDS) PART II

FINAL REPORT

VOLUME I • EXECUTIVE SUMMARY

CONTRACT NO. NAS9-16303
DRL NO. T-1346
DRD NO. MA-664T
LINE ITEM NO. 3

GENERAL DYNAMICS
Convair Division

Kearny Mesa Plant, P.O. Box 80847
San Diego, California 92138
Advanced Space Programs

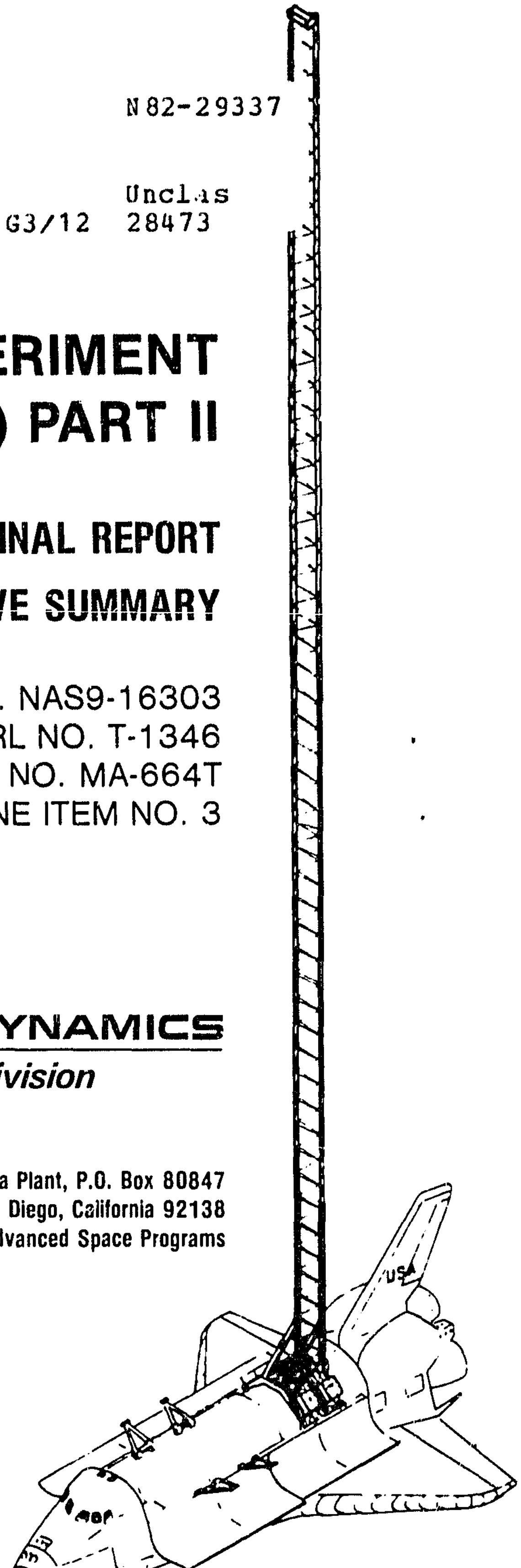

GDC-ASP-82-003
CONTRACT NO. NAS9-16303
DRL NO. T-1346
DRD NO. MA-664T
LINE ITEM NO. 3

SPACE CONSTRUCTION EXPERIMENT DEFINITION STUDY (SCEDS) PART II

FINAL REPORT

VOLUME I • EXECUTIVE SUMMARY

26 April 1982

Submitted to
National Aeronautics and Space Administration
LYNDON B. JOHNSON SPACE CENTER
Houston, Texas 77058

Prepared by
GENERAL DYNAMICS CONVAIR DIVISION
P.O. Box 80847
San Diego, California 92138

PRECEDING PAGE BLANK NOT FILMED

GDC-ASP-82-003

FOREWORD

The final report was prepared by General Dynamics Convair Division for NASA/JSC in accordance with Contract NAS9-1603, DRL No. T-346, DRD No. MA-664T, Line Item No. 3. It consists of two volumes: (I) a brief Executive Summary and (II) a comprehensive set of Study Results.

The principal study results for Part II of the Space Construction Experiment Definition Study (SCEDS) were developed from September 1981 through February 1982, followed by final documentation. Reviews were presented at JCS on 17 December 1981 and 2 March 1982, and at NASA Headquarters on 4 March 1982.

General Dynamics Convair personnel who significantly contributed to the Part II study include:

Study Manager	John Bodle
Control Dynamics	Ray Halstenberg, John Sesak
Preliminary Design	Jim Horne, Bela Kainz, Hans Stocker, Tony Vasques
Avionics & Controls	John Karas, John Sheckelford
System Requirements	John Maloney
System Safety	Steve Douthat, Bill Nagy
Structural Analysis	Bill Bussey, Les Richards, Max Steele
Structural Dynamics	Chris Flanagan, Bob Peller
Mass Properties	Dennis Stachowitz
Economic Analysis	Bob Bradley
Ground Operations	Jim Latham, John Martin, Gary Reichley
Human Factors	Norman Gray
Test Planning	Max Alvarez, Bill Wendt
Advanced Technology	Chuck Claysmith, Bruce Bartholomew

The study was conducted in Convair's Advanced Space Programs Department, directed by D. E. Charhut. The NASA/JSC COR is Lyle Jenkins of the Program Development Office, Clark Covington, Chief.

For further information contact:

Lyle M. Jenkins, Code EB NASA/JSC Houston, Texas 77058 (713) 483-2478	John G. Bodle, MZ 21-9530 General Dynamics Convair Division P.O. Box 80847 San Diego, California 92138 (714) 277-8900, Ext. 2815

PRECEDING PAGE BLANK NOT FILMED

TABLE OF CONTENTS

LIST OF FIGURES

LIST OF FIGURES, Contd

LIST OF TABLES

LIST OF ACRONYMS AND ABBREVIATIONS

A/D	Analog-to-Digital
AFD	Aft Flight Deck
ASE	Airborne Support Equipment
C&W	Caution and Warning
CCD	Charged Coupled Device
CCLS	Computer Controlled Launch Set
CCTV	Closed-Circuit Television
CDR	Critical Design Review
CER	Cost Estimating Relationship
CITE	Cargo Integration Test Equipment
CRT	Cathode Ray Tube
CSDL	Charles Stark Draper Laboratory
CU	Control Unit
CWES	Caution Warning Electric Assembly
DAP	Digital Automatic Pilot
DEU	Display Electronics Unit
DIO	Discrete Input-Output
DRD	Data Requirements Document
DRL	Data Requirements List
EVA	Extravehicular Activity
F/D	Focal Length/Diameter
FSE	Flight Support Equipment
FSS	Flight Support System
F/T	Failure Tolerant
GPC	General Purpose Computer
GSE	Ground Support Equipment
IECM	Internal Environment Contamination Monitor
JSC	Johnson Space Center

LIST OF ACRONYMS AND ABBREVIATIONS, Contd

KSC	Kennedy Space Center
LaRC	Langley Research Center
LSS	Large Space System
MDF	Manipulator Development Facility
MDM	Multiplexer/Demultiplexer
MMSE	Multiuse Mission Support Equipment
MU	Multiplexer
NASA	National Aeronautics and Space Administration
O&C	Operations and Checkout Facility
OPF	Orbiter Processing Facility
OTV	Orbital Transfer Vehicle
PCM	Pulse Code Multiplexer
PDI	Payload Data Interleaver
PDR	Preliminary Design Review
PMP	Parts, Materials, and Processes
PPF	Payload Processing Facility
PRCS	Primary Reaction Control System
PROM	Programmable Read Only Memory
PRR	Preliminary Requirements Review
RAM	Random Access Memory
RCS	Reaction Control System
RMS	Remote Manipulator System
RSS	Rotating Service Structure
SCE	Space Construction Experiment
SCEDS	Space Construction Experiment Definition Study
SIO	Serial Input-Output
SSP	Standard Switch Panel
STP	System Test Plan
STS	Space Transportation System

LIST OF ACRONYMS AND ABBREVIATIONS, Contd

VAB	Vertical Assembly Building
VPF	Vertical Processing Facility
VRCS	Vernier Reaction Control System
WBS	Work Breakdown Structure
WETF	Weightless Environment Test Facility

SECTION 1
INTRODUCTION

1.1 SCOPE

This is the first of two volumes comprising the SCEDS Final Report. It provides an Executive Summary of the study results. Volume II contains the detailed results of all Part II study tasks. This report is the final deliverable contract data item. It satisfies the requirement for Line Item 3 (DRD MA-664T) of DRL T-1346.

1.2 STUDY OVERVIEW

1.2.1 PART I SUMMARY. The Part I study tasks focused on the definition of a baseline Space Construction Experiment (SCE) concept, shown in Figure 1-1.

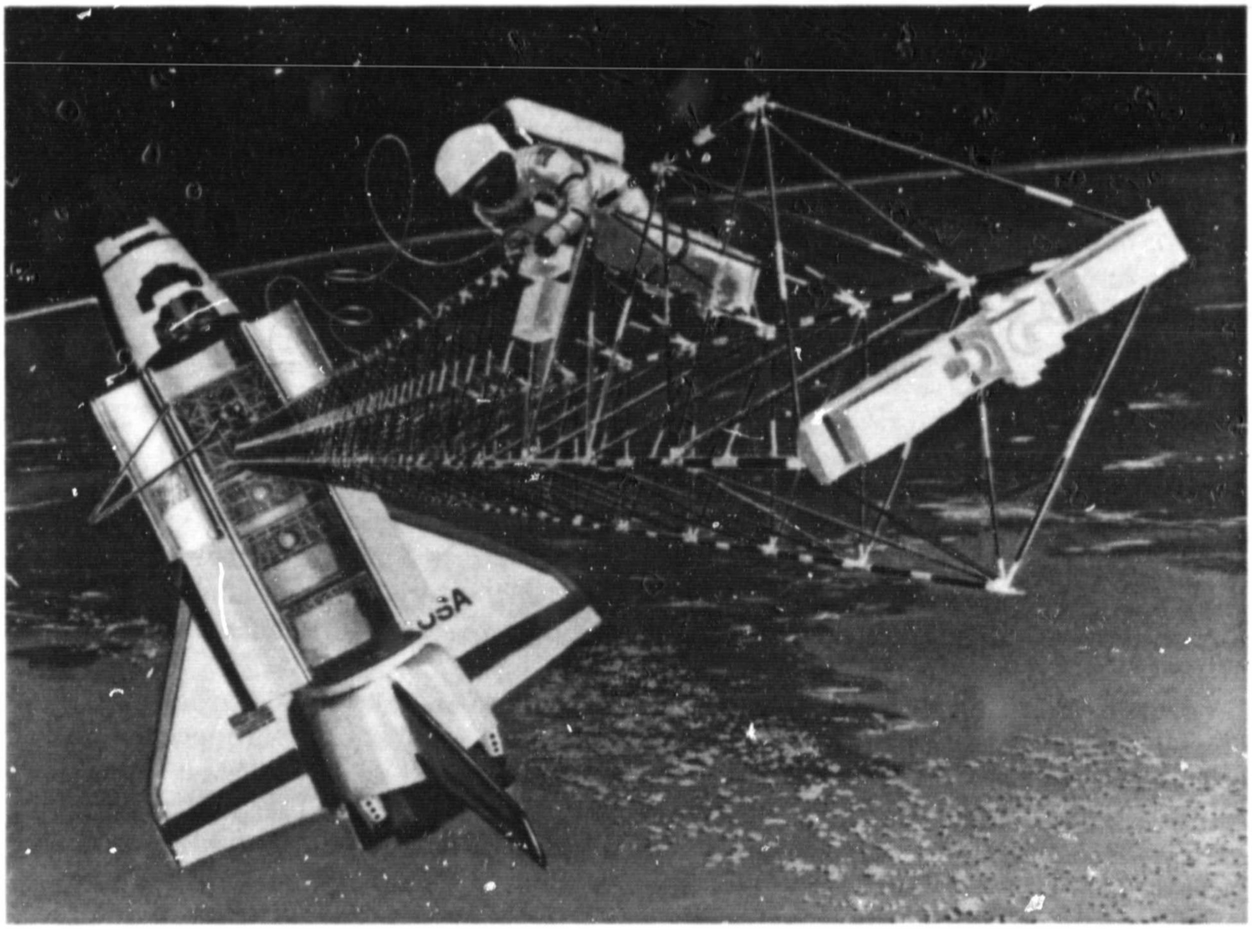

Figure 1-1. Baseline Flight Experiment Concept

The baseline SCE concept incorporated the following characteristics:

a. Test a representative Large Space System (LSS) element. The baseline experiment employs a 50m deployable low natural frequency structure. The structure has a very low coefficient of thermal expansion, achievable through the use of graphite composite materials for construction. Structural dynamic tests provide data to be correlated with math model predictions. Minimal ground testing is to be performed, and minimum flight instrumentation employed. Variable damping augmentation is provided.

b. Share a Shuttle mission with other payloads as a payload of opportunity.

c. Remain attached to the Orbiter throughout the test. Jettison capability is provided; however, the experiment will normally be automatically retracted, restowed, and returned to earth by the Orbiter.

d. Provide options to approach proven flight control capabilities of the Orbiter conservatively and safely exceed proven limits to establish usable capabilities.

e. Exercise a variety of appropriate Large Space System (LSS) construction and assembly operations utilizing basic Space Transportation System (STS) capabilities (EVA, RMS, CCTV, Illumination, etc.) to be correlated with ground tests and simulations.

1.2.2 PART II SUMMARY. After the conclusion of Part I, the study objectives were expanded by NASA/JSC and LaRC to place greater emphasis on the structural dynamics and controls technology aspects of the experiments, and to develop and demonstrate the technologies to meet requirements for large space antenna feed masts. The objectives continued to stress the development of Orbiter capabilities necessary to perform space construction operations.

The initial requirements for Part I of this study resulted in a preliminary design of the experimental structure that incorporated high bending strength to accommodate potential failure modes in the Orbiter Reaction Control System. Cost considerations made it necessary to assume nominal precision in the structural joints and minimum instrumentation. The resulting structural stiffness precluded meaningful Orbiter flight control interaction experiments and the instrumentation system did not address the issues of parameter identification.

The Part II requirements specified a larger, more flexible, high-precision, 100m long, deployable structure. More extensive instrumentation was incorporated to facilitate parameter identification and verify tip motion. A flexible base mount was added to allow the Orbiter Digital Automatic Pilot (DAP) performance to be verified near its control limits. Ground test and flight test programs were defined in greater detail. Payload integration interfaces and safety requirements were also defined and analyzed.

The Part II study activities were divided into five major tasks which were interrelated as shown in Figure 1-2.

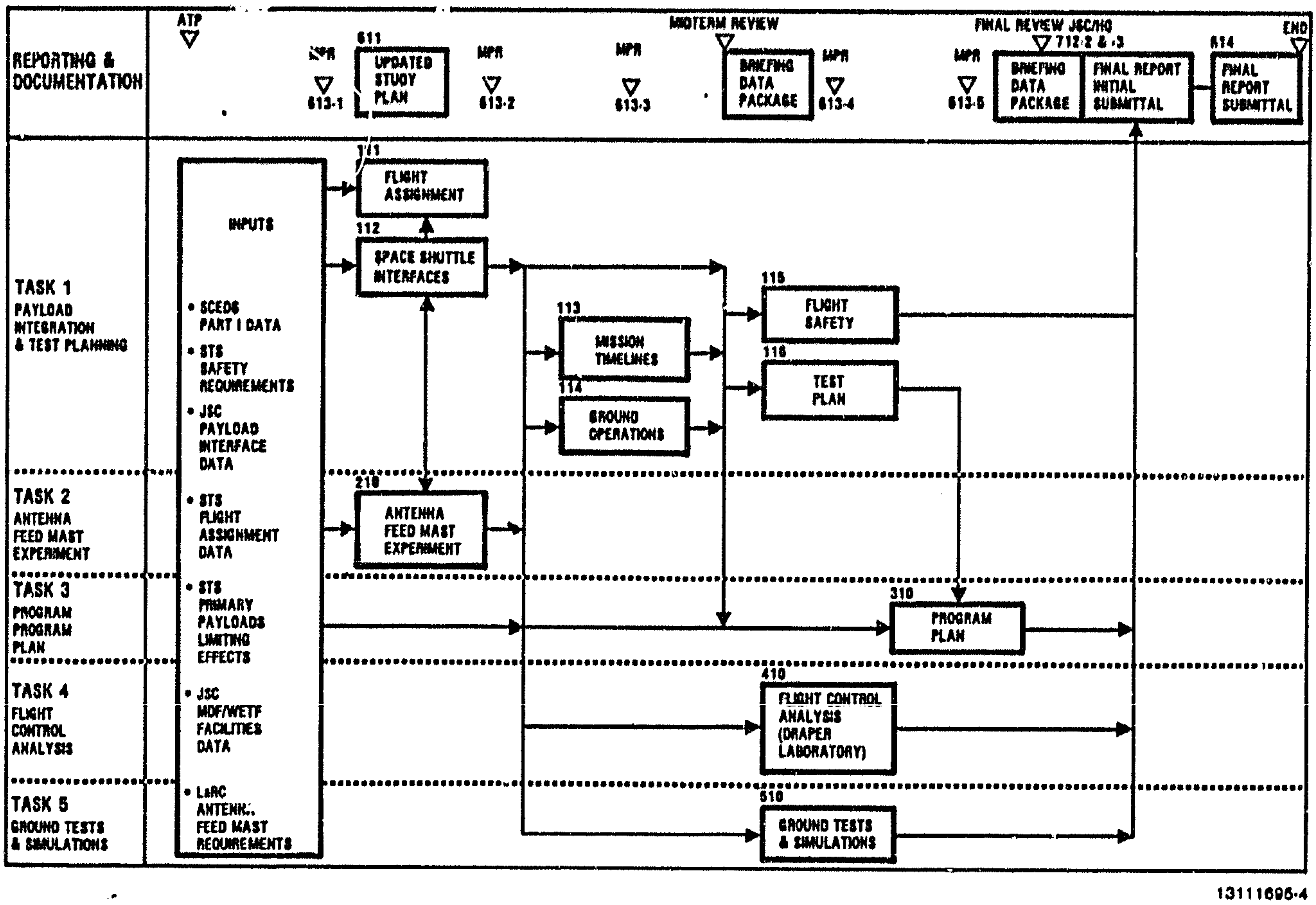

Figure 1-2. SCEDS Part II Task Relationships

Task 1 further developed and defined the SCE for integration into the Space Shuttle. This included development of flight assignment data, revision and update of preliminary mission timelines and test plans, analysis of flight safety issues, and definition of ground operations scenarios.

Task 2 incorporated new requirements for the flight experiment and defined changes to satisfy these requirements for a large space antenna feed mast test article, as well as more detailed structural dynamics and controls experiments.

Task 3 expanded and updated the Part I preliminary program plan and cost estimates based on the revised preliminary design data and test plan.

Task 4 revised SCE structural dynamic characteristics for simulation and analysis of experimental tests by the Charles Stark Draper Laboratory to define control limits and interactions effects between the SCE and the DAP.

Task 5 defined the approach and test methods to conduct ground tests and develop simulations for predicting flight test performance of the structural test article, Orbiter flight control system, and EVA/RMS construction operations.

SECTION 2
STUDY RESULTS

Study results of SCEDS Part II are summarized in the following subsections. These include flight experiment test article definition, preliminary design and analysis, DAP interactions, excitation and instrumentation, test plan and programmatics.

2.1 FLIGHT EXPERIMENT TEST ARTICLE

2.1.1 FEED MAST STRUCTURAL REQUIREMENTS. The structural requirements for the feed mast test article as established by NASA/LaRC are shown below. The goal was to achieve a mast structure which fell within size and stiffness parameters considered appropriate for large space antenna feed mast structures.

a. Size: Length = 100m
   Depth = 1.8 to 2.8m

b. Stiffness: Approximately 2×10^7 N-m^2

c. 0.05 to 0.10 Hz cantilever first mode natural frequency

d. Tip position criteria: ±10 cm longitudinal deviation
   ±10 cm combined rotation/translation

e. Linear compaction ratio: $\frac{\text{deployed length}}{\text{stowed length}} = 20$ to 25

f. Test article to withstand vernier RSC in lieu of primary RCS loads.

2.1.2 FEED MAST CANDIDATES. Potential feed mast candidates (Figure 2-1) were compared before defining the feed mast test article. The selected mast structure was then sized and analyzed for dynamic performance.

The diamond truss has advantages which make it most suitable for an experimental program.

a. Its low volume packaging requires less cargo space in the Shuttle Orbiter payload bay which allows it to "piggyback" other palletized payloads.

b. Its single failure tolerant structure is an important safety consideration because of the potential for damaging thin walled slender struts during EVA and RMS activities.

c. The all-rigid-strut construction provides greater confidence that the structural properties will remain as modelled throughout ground and flight testing.

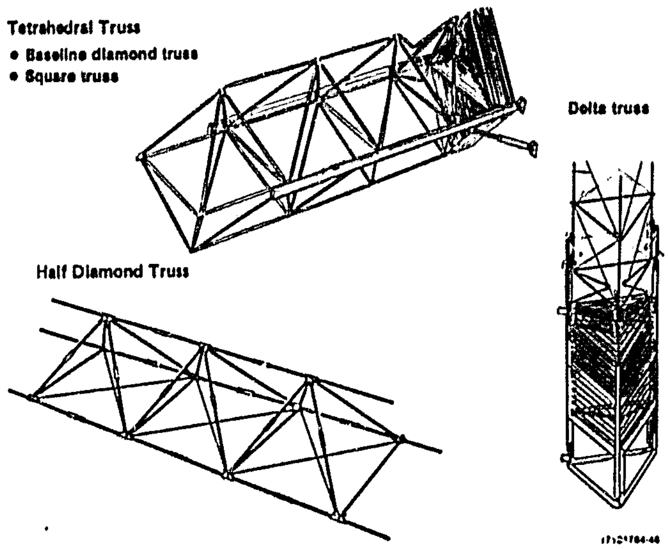

Figure 2-1. Feed Mast Structural Candidates

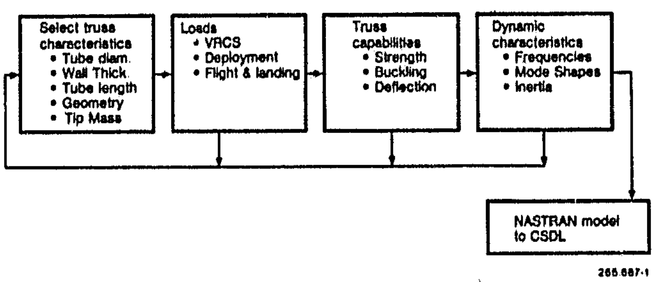

Figure 2-2. Mast Structural Sizing Analysis Flow

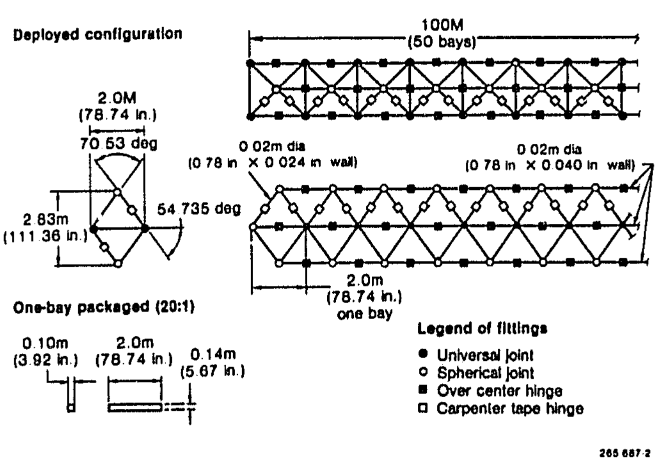

Figure 2-3. Revised Tetrahedral Diamond Truss Geometry

A decision to continue using the diamond truss for the experiment structure was supported by an analysis to verify that it could meet the structural and dynamic requirements for a feed mast. This is an iterative process as illustrated in Figure 2-2.

2.1.3 STRUCTURAL AND DYNAMIC CHARACTERISTICS. The revised geometry of the diamond truss is shown in Figure 2-3. The effects of the preliminary sizing analysis using a 250 kg tip mass are as follows:

a. Width increased 0.39m

b. Height increased 0.55m

c. Linear packaging ratio increased from 8.7:1 to 20:1

d. Diameter of longitudinal members decreased 0.025m

e. Length increased 49.9m

f. Stiffness (EI) in pitch decreased to 2.0×10^7 N·m^2

g. Stiffness (EI) in roll decreased to 1.3×10^7 N·m^2

It was concluded that a flexible base mounting for the flight experiment truss was the best approach to reducing the first mode bending frequency to less than 0.05 Hz to provide a challenge to the DAP.

The frequencies for the first six modes are listed in Table 2-1 for two different tip masses with both flexible and rigid support. These four configurations were submitted to CSDL to obtain comparative results on their effects on the DAP.

Table 2-1. Diamond Truss Structural Dynamic (Orbiter-attached Free-Free) Characteristics

Mode	Description	Frequencies (Hz)			
1	1st pitch bend	.0390	.0861	.0391	.1192
2	1st roll bend	.0618	.1138	.0533	.1322
3	2nd roll bend	.6716	.9350	.6677	.9586
4	2nd pitch bend	.8069	1.1783	.8116	1.2092
5	3rd roll bend	2.2826	2.8937	2.2678	2.8298
6	1st torsion	2.7943	3.1956	2.7901	3.1956
	Tip mass (kg)	250	250	100	100
	Support stiffness (n/m)	1.55×10^5	∞	$.75 \times 10^5$	∞

02032178-19

2.2 PRELIMINARY DESIGN

2.2.1 SCE SUPPORT STRUCTURE.

The SCE support structure (Figures 2-4 and 2-5) was changed to incorporate a spring mounting arrangement for the deployable truss assembly. Drives and mechanisms are provided to allow the springs to be locked out during truss dynamic tests.

The truss assembly is mounted on a rigid frame which is pivoted about the roll axis. Two leaf springs reacting against the roll frame provide a truss mounting stiffness of 1.55×10^5 N-m/rad in roll. Each of the two pitch support struts has a spring cartridge to give the same stiffness in pitch as in roll.

The pitch strut spring cartridges are locked or unlocked by gear motors that actuate ball detent locking mechanisms. The roll frame is rigidly locked to the support structure by two motor driven locking pins.

An RMS actuated forward holddown latch is provided to secure the folded truss to the roll frame for flight.

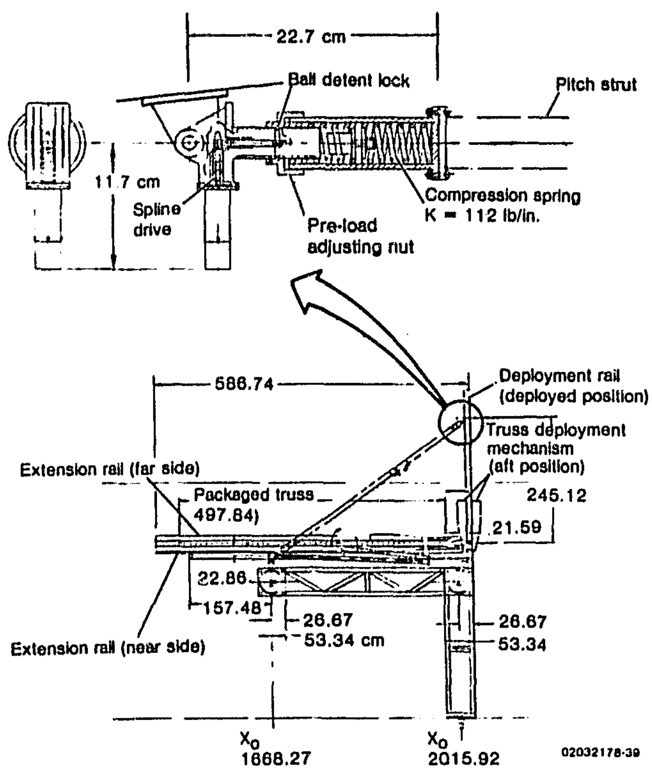

Figure 2-4. Support Structure and Pitch Start Mechanism

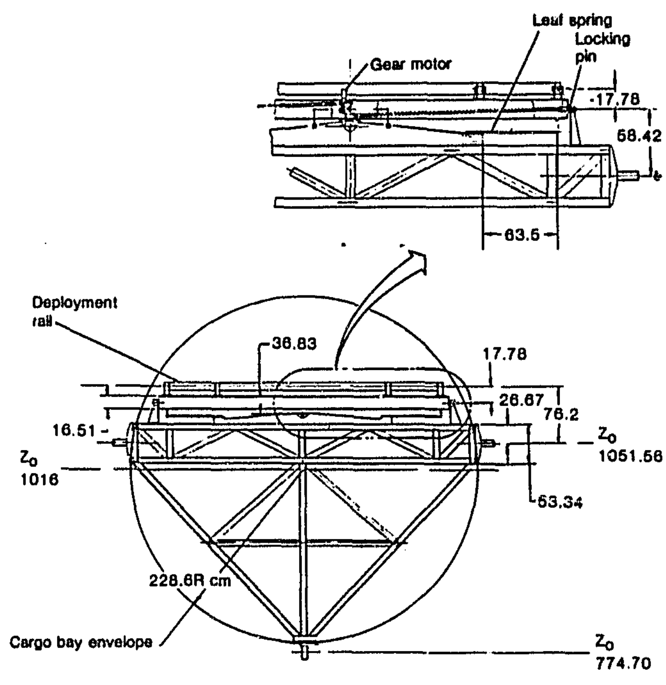

Figure 2-5. Support Structure and Roll Frame Mechanisms

ORIGINAL PAGE IS
OF POOR QUALITY

2.2.2 DEPLOYABLE TRUSS. The updated general arrangement of the deployable truss (Figure 2-6) shows the initial stage of the truss deployment with upper and lower lateral struts unfolded and the first two bays deployed. The system consists of a truss deployment rail structure with extension rails, two motorized carriages, two electric cable take up reels, and the deployable truss with a tip-mounted damping augmentation unit and mass. The rails contain tracks for the truss and carriage rollers and gear racks for the carriage drive pinion. The automatically controlled carriages deploy and retract the truss linearly. Secondary deployment operations are performed by the RMS as defined in Part I of the study.

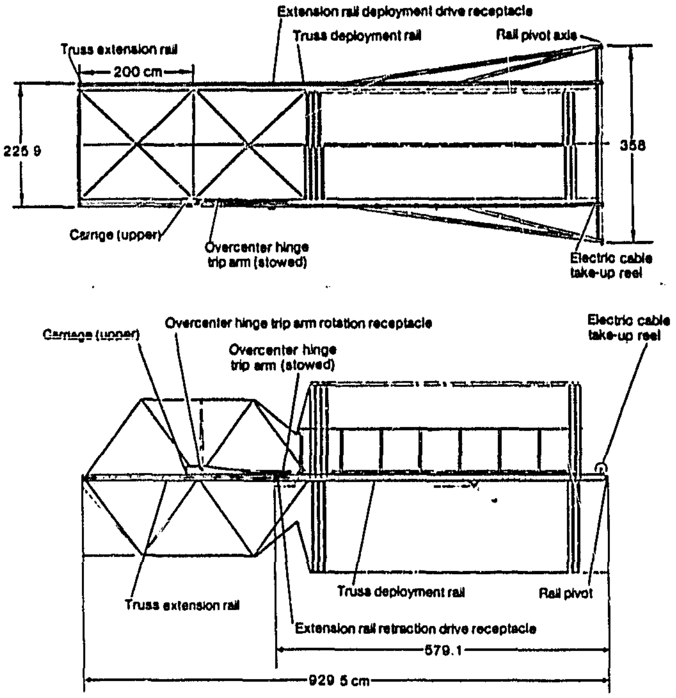

Figure 2-6. Truss General Arrangement

The end of the deployable truss is equipped with a special support frame for the damper sets and tip mass (Figure 2-7). Two steel bars are attached to the support frame, each by an explosive bolt. The steel bars provide the added mass necessary to bring the total weight of the tip package to 250 kg. However, the tip masses must be jettisoned to provide a favorable center of gravity of the experiment for payload jettison in the event of a retraction failure of the truss.

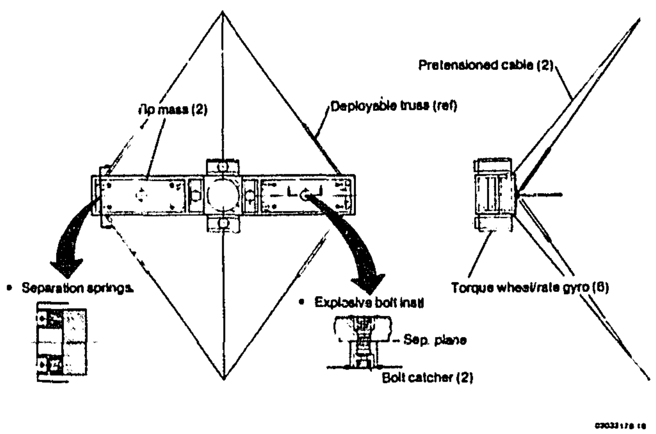

Figure 2-7. Damping, Excitation and Tip Mass Assembly

2.2.3 SCE CONTROLS. The hard-wire control concept defined in SCEDS Part I was updated as shown in Figure 2-8 to incorporate the following changes:

a. The Control Unit (CU) was relocated from the Aft Flight Deck (AFD) to the SCE support structure in the cargo bay.

b. The dedicated payload AFD control panel was eliminated. The Orbiter-provided standard switch panel (SSP) will be used to control the operation of the SCE. The Orbiter-provided active latch controls will be used for jettison control, and the Orbiter-provided cathode ray tube (CRT) display and keyboard will be used for monitoring status and data.

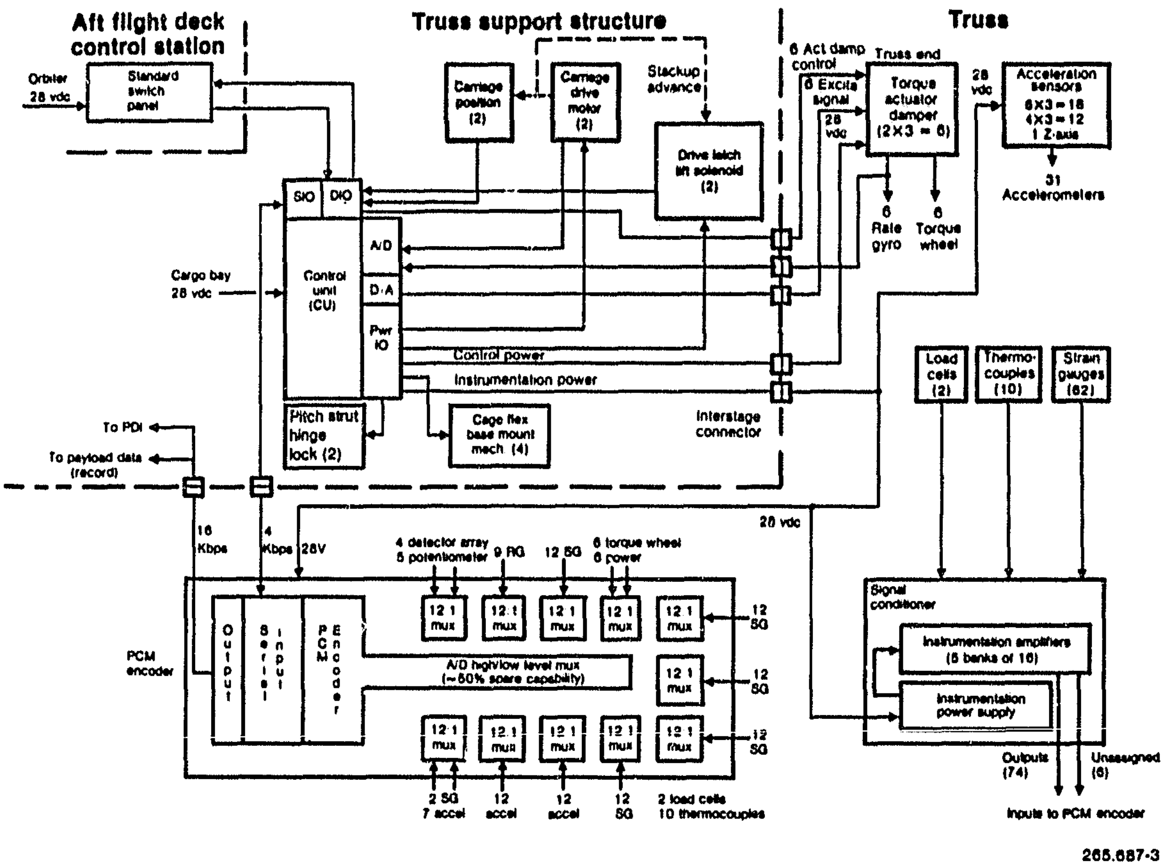

Figure 2-8. SCE Updated Control and Instrumentation

c. Dual PCM outputs provided direct payload data interlevel (PDI) and payload recorder interfaces. This will allow data to be recorded and/or downlinked in real time.

d. Mechanical controls for caging and release of the flexible base mount springs and unlatching pitch strut hinges were added.

e. Instrumentation was updated and separate units for PCM encoder and signal conditioner were defined.

2.2.4 SHUTTLE ORBITER/SCE INTERFACES. The interfaces and interface hardware requirements for the SCE integrated with the Space Shuttle system were identified and defined. The display and controls interfaces are summarized in Figure 2-9. The SCE support structure employs a standard five point payload retention system with four longeron attachments (Figure 2-10) and one keel fitting attachment (Figure 2-11). Active longeron and keel fittings are Orbiter provided to allow jettison of the payload with the RMS.

A standard connector panel hard-mounted to a mid-fuselage frame as shown in Figure 2-11 will be used for the payload interfaces for power, data, and control harness connections. The Orbiter harnesses connect to this panel. The SCE payload includes a set of lanyard pull-type connectors designed to separate during jettison.

ORIGINAL PAGE IS
OF POOR QUALITY

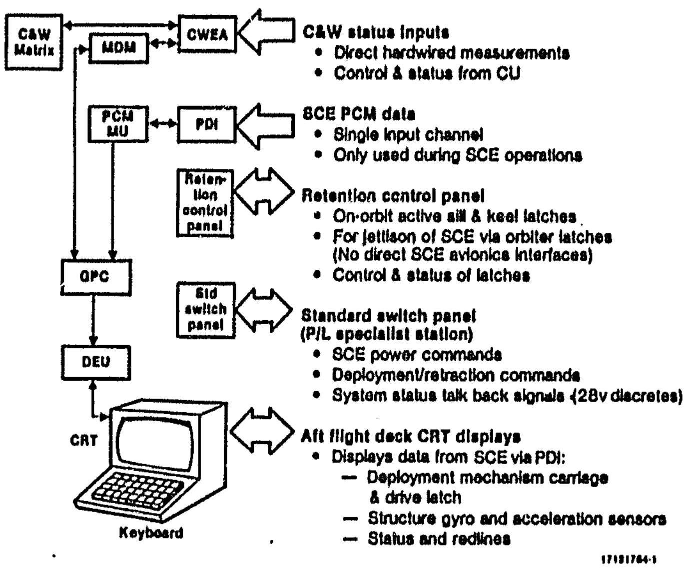

Figure 2-9. Display and Controls Summary

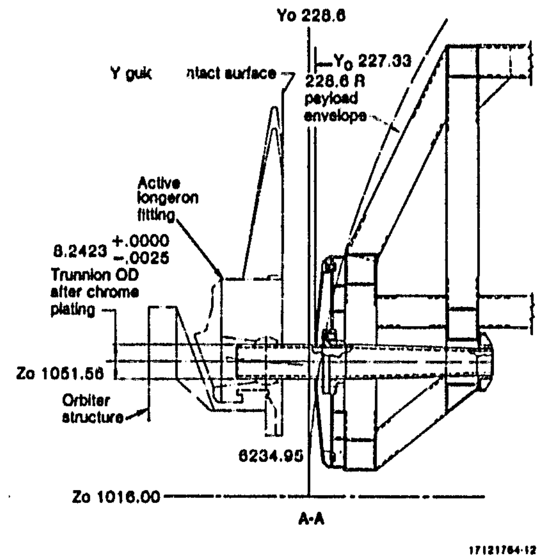

Figure 2-10. SCE Payload Retention Longeron Attachment

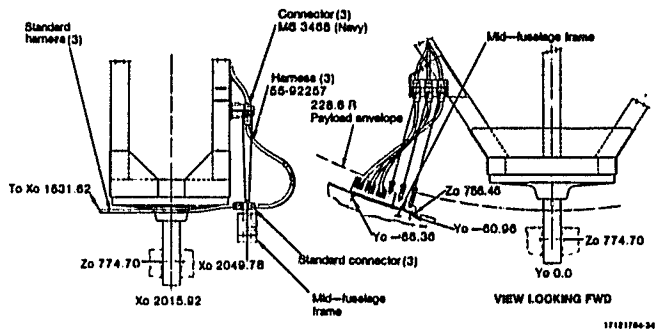

Figure 2-11. Payload Power, Data and Control Harness Interface

Table 2-2. Truss Support Loads

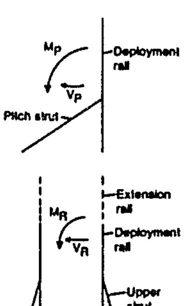

Support structure Element	loads	Maximum value	Deployed length	Applied loads	
Pitch loads				M_P (N·m)	V_P (N)
Pitch strut	Axial	430N	50 bays/100m	1671	18
Deployment Rail	Axial	260N	50 bays/100m	1671	18
	shear	405N	49 bays/98m	1620	17
	moment	364N-m	34 bays/68m	878	13
Roll loads				M_R (N·m)	V_R (N)
Upper strut	Axial	1065N	30 bays/60m	626	11
Lower strut	Axial	645N	50 bays/100m	943	10
Deployment Rail	Axial	717N	50 bays/100m	943	10
	shear	210N	49 bays/98m	931	10
	moment	121 N-m	44 bays/88m	820	10

2.3 DESIGN ANALYSIS

2.3.1 STRUCTURAL ANALYSIS.

Deployment rail loads were computed for the new deployable truss configuration with a 250 kg tip mass. Shear and moment loads applied in pitch and roll were determined for the VRCS thrusters "on" case. The maximum loads summarized in Table 2-2 vary with deployed length due to the relative positions of the truss deployment support rollers in the rails. These maximum loads were determined to be well within the structural capability of the rails.

Truss loads for the revised truss configuration with a 250 kg tip mass and VRCS control moments applied by the Orbiter were determined to be very low, as seen in Figure 2-12. The slender struts used in the structure were determined to be compatible with the maximum loads indicated. The truss struts are manufactured from either a GY70/934 graphite epoxy material or a Pitch 75 type fabric to provide the high modulus in the

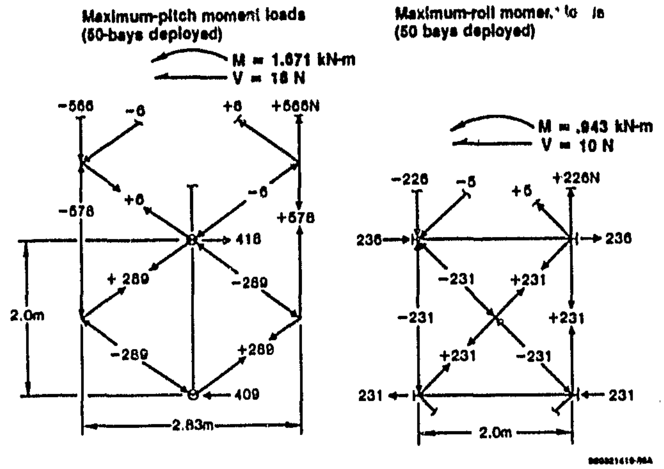

Figure 2-12. Revised Truss Loads

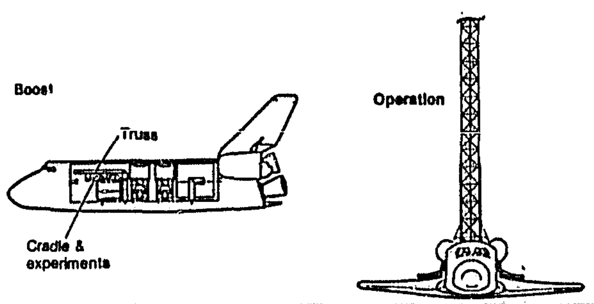

Item	Weight (kg)
Tip-mass	250
Truss	177
Cradle	657
Experiments	91
Total	1,175

Deployed phase	Center of mass (m)			Moment of inertia (kgm^2)		
	X	Y	Z	I_{xx} (Roll)	I_{yy} (Pitch)	I_{zz} (Yaw)
1/3	19.96	0	17.17	10.74×10^4	10.78×10^4	1.83×10^3
2/3	19.96	0	26.97	6.36×10^5	6.37×10^5	1.83×10^3
Full	19.96	0	38.74	1.59×10^6	1.59×10^6	1.83×10^3
Jettison tip-mass	19.42	0	27.2	7.64×10^5	7.65×10^5	1.2×10^3

Figure 2-13. Revised Mass Properties

laminated tubes ($E = 20 \times 10^6$ psi) required to minimize wall thicknesses for reduced cost and weight. The graphite epoxy material also provides the near-zero CTE required for thermal stability of the truss structure.

2.3.2 MASS PROPERTIES. Mass properties for the revised experiment were calculated as shown in Figure 2-13. The moments of inertia are given relative to the Orbiter coordinates. The mass properties of the Orbiter are not included.

2.3.3 SAFETY ANALYSIS. A preliminary phase 0 safety analysis (Figure 2-14) of the SCE was conducted to identify the potential hazards based on the preliminary design data. This analysis forms the basis for identifying safety critical requirements for the experiment final design phase, and assessing the adequacy of the preliminary design in conforming to Shuttle payload safety requirements. The two failure tolerant functions that were identified are basically compatible with the controls subsystem concept.

The criticality of the structure to the safety of the Orbiter points to the need for very high standards of quality and materials controls. These items will have substantial cost impact on the flight structure. However, they are also necessary to achieve the modeling accuracies required for large space structures.

2.4 DIGITAL AUTOPILOT/STRUCTURE INTERACTIONS

The DAP simulations are run at The Charles Stark Draper Laboratory (CSDL) using structual dynamics data supplied by Convair. Late in Part I, data for a 50m structure with a flexible mount was developed and transmitted to CSDL, but the simulation results were not available in time to be included in the Part I Final Report. The structure had a 400 kg tip mass and a mounting spring constant of 1.0×10^5 N-m/rad. A time history from the CSDL simulation is shown in Figure 2-15. At the start of the run, a 10-degree roll maneuver at

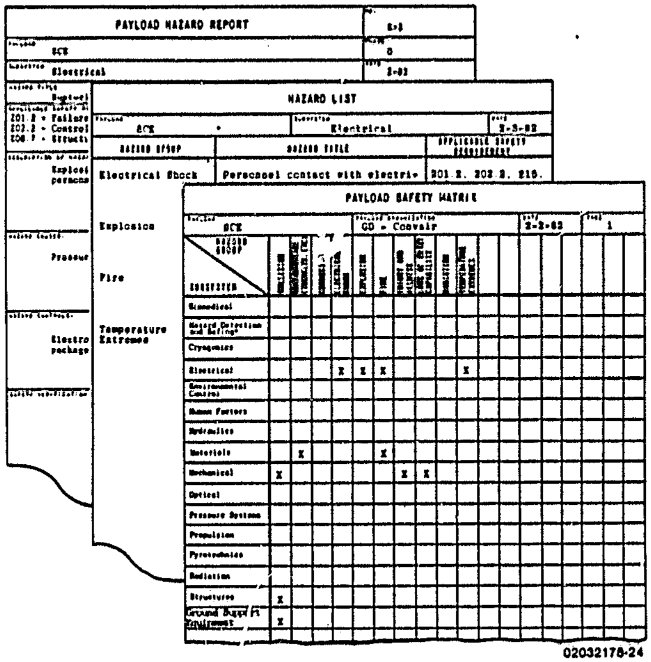

Figure 2-14. Phase 0 Safety Analysis Performed

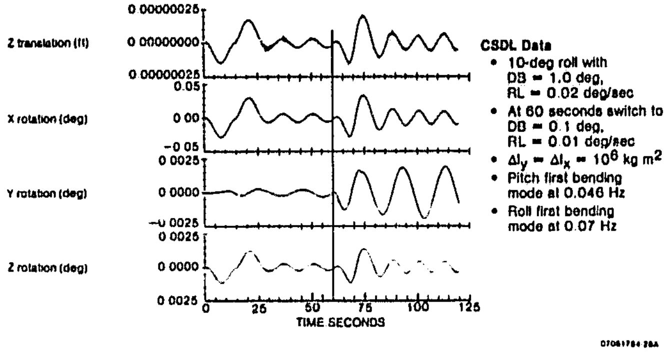

Figure 2-15. Interaction of Flexible Structure and the DAP

0.2 deg/sec is commanded with the phase plane rate limit (RL) set at 0.02 deg/sec and the attitude deadband (DB) at 1.0 degree. (The traces are for the flexible body only, before the rigid body response is added.) Vernier Reaction Control System (VRCS) activity is indicated by the high frequency on the Z translation trace at the top.

When the phase plane parameters are tightened at 60 seconds, the VRCS firings are seen to persist and the small amplitude Y rotation (pitch) does not seem to be damping out. Since the run is too short to fully characterize the pitch behavior, additional investigations are required.

Subject to a more detailed pitch axis evaluation, the characteristics shown in Figure 2-15 appear to be very desirable. Normal operations can be carried out with the initial phase plane limits and the DAP behavior will be essentially nominal, but tightening the limits challenges the DAP and provides off-nominal behavior for the structural interaction evaluation.

<u>There is absolutely no intent to operate close to any DAP instability</u> but rather to achieve sufficient off-nominal operation to permit an evaluation of the structural modeling and DAP simulation as they apply to Orbiter-attached large space structures.

2.5 STRUCTURAL DYNAMICS EXPERIMENTS

2.5.1 <u>EXPERIMENT MODAL EXCITATION</u>. To investigate the dynamics of a low-frequency structure, it is necessary to provide both suitable low frequency excitation and compatible instrumentation. These areas were analyzed by choosing three excitation techniques for evaluation: Orbiter reaction control system (RCS) firings, a mass explusion thruster system at the tip of the structure, and torque wheels. A 100m structure with a 1000-kg tip mass was selected for this analysis based on availability of suitable dynamic data. The Orbiter-attached structure was then evaluated for the relative response of the first three pitch free-free bending modes. These first three modes had frequencies of 0.072, 0.92, and 3.0 Hz, respectively. Since the relative modal response is dependent on the type of measurement to be made, acceleration, velocity, and displacement were considered for both linear measurements (mode shape) and angular measurements (slope). The results are presented in Table 2-3.

Table 2-3. Relative Modal Excitation from Alternative Techniques – Pitch Modes Only

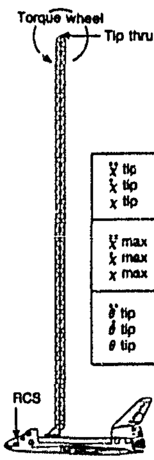

	Normalized gain						
		RCS firings		Tip thruster		Torque wheel at tip	
	Mode 1	Mode 2	Mode 3	Mode 2	Mode 3	Mode 2	Mode 3
$\ddot{x}$ tip	1.00	.021	0.004	0.054	0.018	2.12	2.12
$\dot{x}$ tip	1.00	0.0016	0.0001	0.0042	0.0004	0.164	0.051
x tip	1.00	0.0001	2×10^{-6}	0.0003	10^{-5}	0.013	0.0012
$\ddot{x}$ max	1.00	0.431	0.135	1.126	0.654	43.66	75.66
$\dot{x}$ max	1.00	0.033	0.0033	0.087	0.016	3.39	1.83
x max	1.00	0.0026	0.0001	0.0068	0.0004	0.26	0.044
$\ddot{\theta}$ tip	1.00	0.810	0.436	2.12	2.12	82.1	245.2
$\dot{\theta}$ tip	1.00	0.063	0.011	0.164	0.051	6.40	5.94
θ tip	1.00	0.0049	0.0003	0.013	0.0012	0.49	0.144

070623314

All values have been normalized to the first mode. For example, with RCS firings, the maximum displacement (x max) of the third mode is seen to be 0.0001 times the maximum displacement of the first mode. Thus, it appears that attempts to gather data from the higher modes by firing the RCS and taking displacement measurements (as might be taken by an optical system) will encounter problems in extracting the third-mode signal from the first-mode noise.

Inspection of the table indicates that the RCS tends to excite mostly the first mode; that the thruster at the tip is somewhat better than the RCS for higher mode excitation; and that a torque wheel at the tip is by far the best of the techniques for providing reasonably uniform modal excitation. Based on this data, the torque wheel has been chosen for a multimode random shake wherein the data is recorded for later ground determination of frequencies, mode shapes, and damping ratios. Rate gyros and accelerometers have been chosen for instrumentation based on availability and reasonable dynamic range requirements between modes.

The result that the RCS excites mostly the first mode was used to define another test. Since the random shake data reduction will provide linearized data to the exclusion of nonlinear structural effects, the RCS will be used to excite the first mode and data will be taken as the oscillation amplitude decays. Thus, structural behavior may be evaluated over a range of amplitudes so as to define nonlinear behavior, especially damping. Analysis indicates that the oscillation, motion amplitude can be controlled by firing the VRCS for half of a first-mode period. Each such firing introduces about ±0.2m of tip motion so the oscillation may be "pumped up" to any predetermined amplitude by repeated timed firings.

2.5.2 JOINT CLEARANCE EFFECTS. Another area that can be investigated by use of the flight experiment is joint damping effects. Energy loss in joints is usually a significant portion of structural damping, and only by going into space can the joints be realistically loaded as they will be on operational space structures.

A concept for inducing clearance fits in a number of the test truss joints is shown in Figure 2-16. The eccentric pins in an expandable bushing would maintain zero clearance fit in each test joint until the pins are rotated either by remotely activated cables or by manual EVA action. The first mode, pitch bending, frequency-free decay characteristics, with and without unloaded test joints, would be compared.

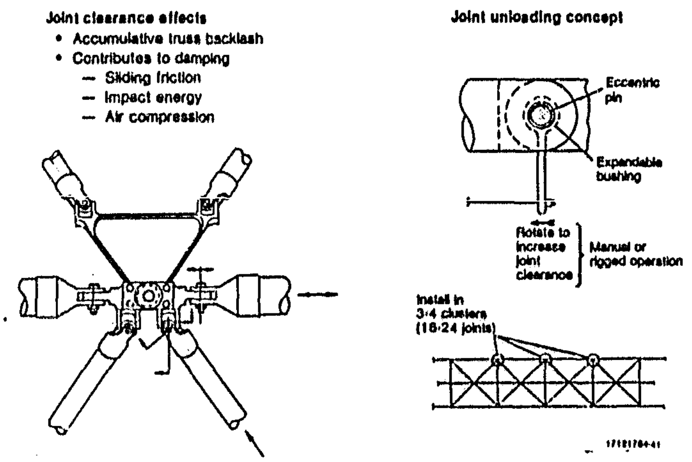

Figure 2-16. Joint Clearance Effects Test Concept

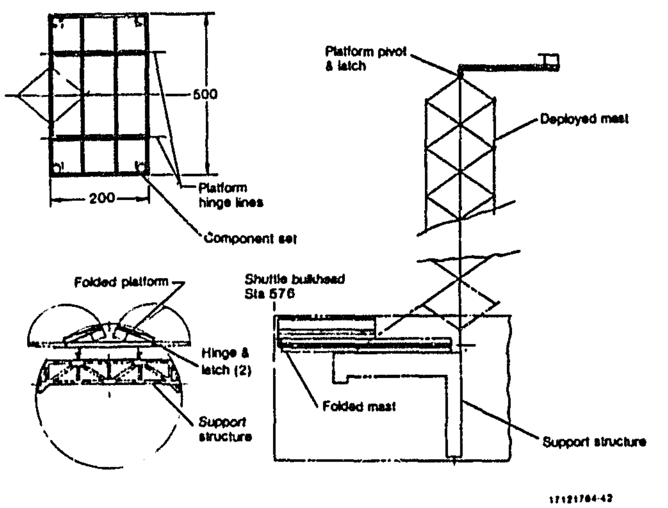

Figure 2-17. Feed Array Platform Concept

2.5.3 CLOSELY SPACED MODES. A mast will have a sparsely populated modal spectrum. A "feed array" platform concept (Figure 2-17) was designed to provide the modal density which is typical of antenna reflectors. With two closely-spaced modes at about 0.2 Hz and three closely-spaced modes near 0.7 Hz, the frequencies of a large reflector could be matched but the masses and mode shapes would be different. Four torque wheel damper sets would be installed on the platform to permit multimodal excitation for test and post excitation modal damping.

2.5.4 SUMMARY OF OPTIONS. Selected areas of structural dynamics and control are indicated in Table 2-4. Investigation with the "feed array" platform structure has not been selected since closely-spaced mode control issues can be addressed on the ground.

2.5.5 INSTRUMENTATION. The SCE will be instrumented to identify and accurately quantify mode shapes and modal frequency response of the first six modes of the test truss attached to the Orbiter in space free flight. This will require measuring linear and angular displacements and rates at selected stations along the structure,

Table 2-4. SCE Control and Dynamics Options

Excitation/Test Method	Structural Dynamic and Control Issues: Linear Dynamics	Nonlinear Behavior	DAP Interactions	Control Device Demo	Identification and Control of Complex Modes
Orbiter Maneuvers (RCS)					
Pitch	✓	(✓)	(✓)	(✓)	
Roll	✓	✓	(✓)	(✓)	
Yaw	✓	✓	✓	✓	
Torque Wheel Random Shake	(✓)			(✓)	
Sinusoidal Torque Wheel	✓	✓		✓	
RCS on Mast Tip	✓	✓			
"Feed Array" Structure	✓			✓	✓
Variable Joint Clearance		(✓)			

(✓) Selected Options.

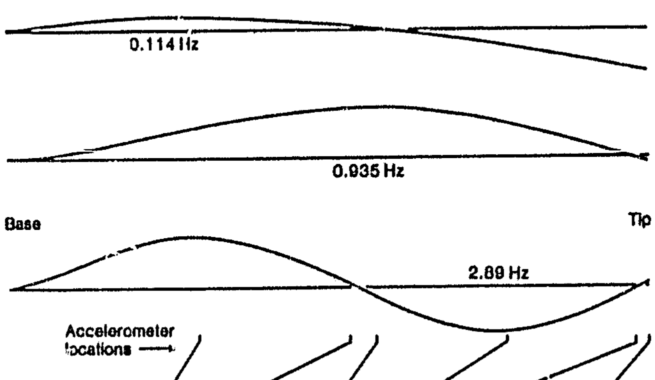

Location meters	30	54	58	78	88	100
1st roll	-31.7	-8.3	-1.3	42.2	94.6	100
2nd roll	61.1	99.6	100	60.6	0.1	-7.7
3rd roll	100	1.2	-2.4	-92.5	-8.9	4.5

Percent of maximum displacement

02032178 22

Figure 2-18. Roll Bending Mode Shape Instrumentation

as well as Orbiter motions and the relative motion between the structure and the Orbiter interfaces. The linear displacement of the tip of the test truss relative to the base of the truss will also be measured to verify the precision with which relative tip motion can be maintained.

The mode shapes for the first three roll bending modes of the structure are shown in Figure 2-18. Although the Orbiter is quite massive when compared to the structure, it responds to change the first mode from the classical cantilever shape. The servo-accelerometer placement shown covers all maximums and provides two measurements at all nodes. Two measurements near a node permit interpolation to more accurately locate the node point. Pitch modes are similarly measured using the same stations. Rate gyros at the tip and at 78m above the base provide required slope data.

Concepts for measuring tip motion are shown in Figure 2-19. The Concept 2 laser/detector array system was baselined pending more detailed analysis of cost and availability of options.

Measurement of SCE support pin loads and deflections (Figure 2-20) will allow the deflections of the support structure to be computed from its structural model.

The raw data from the Orbiter rate gyros will be available in downlist for measuring Orbiter motions. This will require an off-line ground support system to format the data into pitch, yaw and roll rates.

2.6 PRELIMINARY SYSTEM TEST PLAN

2.6.1 TEST PROGRAM SUMMARY.

The test program flow diagram (Figure 2-21) describes an orderly progression to meet the SCE program objectives and requirements. The development testing phase will allow system manufacturing and design problems, and math modeling uncertainties, to be evaluated and resolved during the design phase. The component qualification testing will verify that

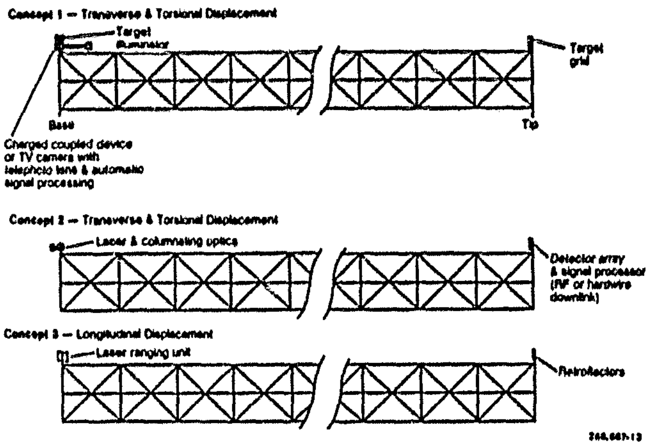

Figure 2-19. Tip Motion Measurement Concepts

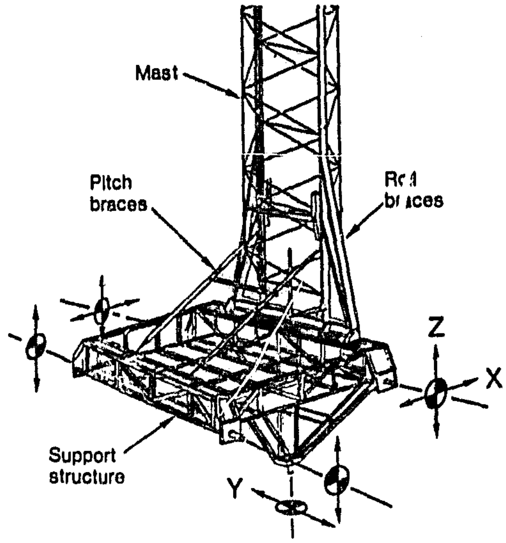

Figure 2-20. Forces at the Orbiter Interfaces

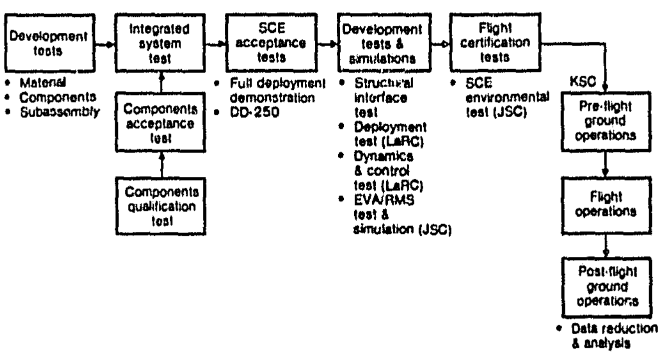

Figure 2-21. SCE Test Program Flow Diagram

no critical weaknesses exist before subsystem and system level tests are initiated. The flight certification tests will verify the flight worthiness, environmental compatibility, and functional capability of the integrated SCE.

A simulation and ground test program plan which would fully develop modeling techniques for flight performance predictions would include the elements shown in Figure 2-22. The initial structural dynamics model will derive data on struts, joints, fittings, mass properties, etc., from the component tests. The model will be tested by performing subassembly tests of the modeled 5-bay structural segment. Structural interface tests of the flight experiment support structure will allow interface deflections at the base of the truss to be computed from measured flight loads. Deployment tests and dynamics and controls tests will allow the structural dynamic and control models for the flight test article to be evaluated and provide a data base for evaluating the effectiveness of ground test of partially deployed configurations in ensuring accurate flight test performance predictions.

The EVA and RMS ground tests and simulations will be conducted in two phases. One-g tests and simulations will be performed on the SCE installed in the JSC Manipulator Development Facility (MDF)(Figure 2-23). Water buoyancy zero-g simulations and tests on a test segment of truss will be conducted in the JSC Weightless Environment Training Facility (WETF) (Figure 2-24).

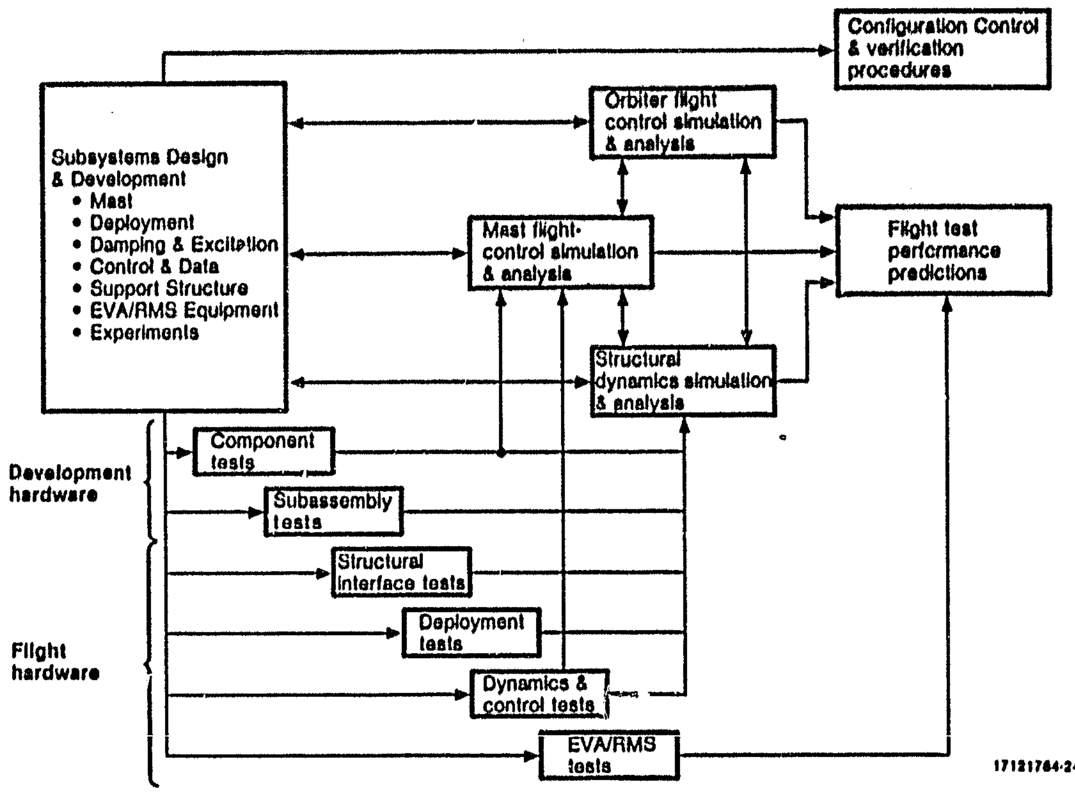

Figure 2-22. Ground Test and Simulation Approach

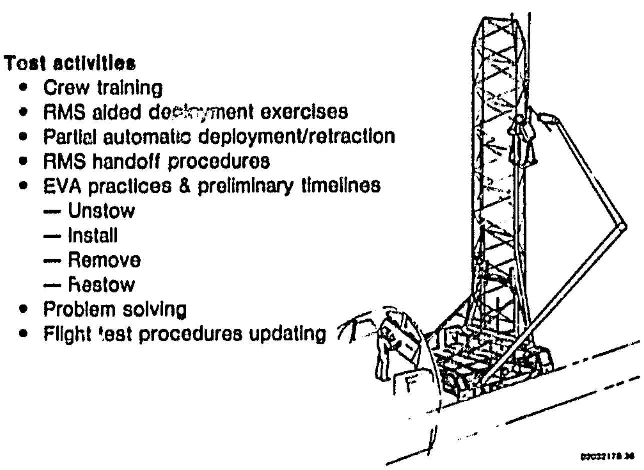

Figure 2-23. MDF Tests and Simulations Concept

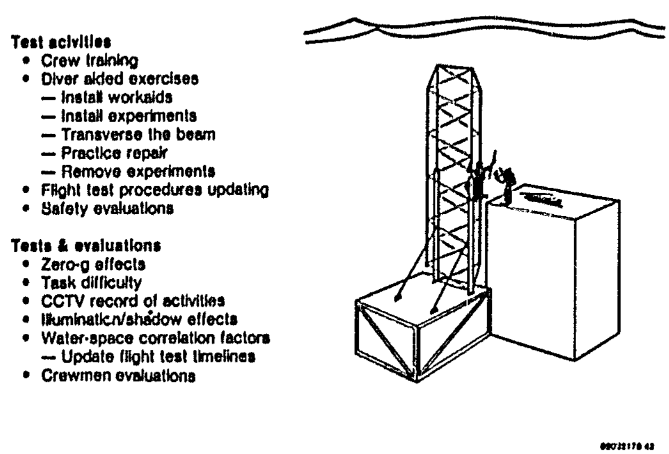

Figure 2-24. WETF Simulations and Test Concept

Ground operations flow at KSC will be as shown in Figure 2-25. Initial preflight operations will be performed in a Payload Processing Facility (PPF) to be designated for SCE use. PPF tasks include receiving and inspection, refurbishment, preparation, and checkout operations as necessary to establish SCE system

ORIGINAL PAGE IS OF POOR QUALITY

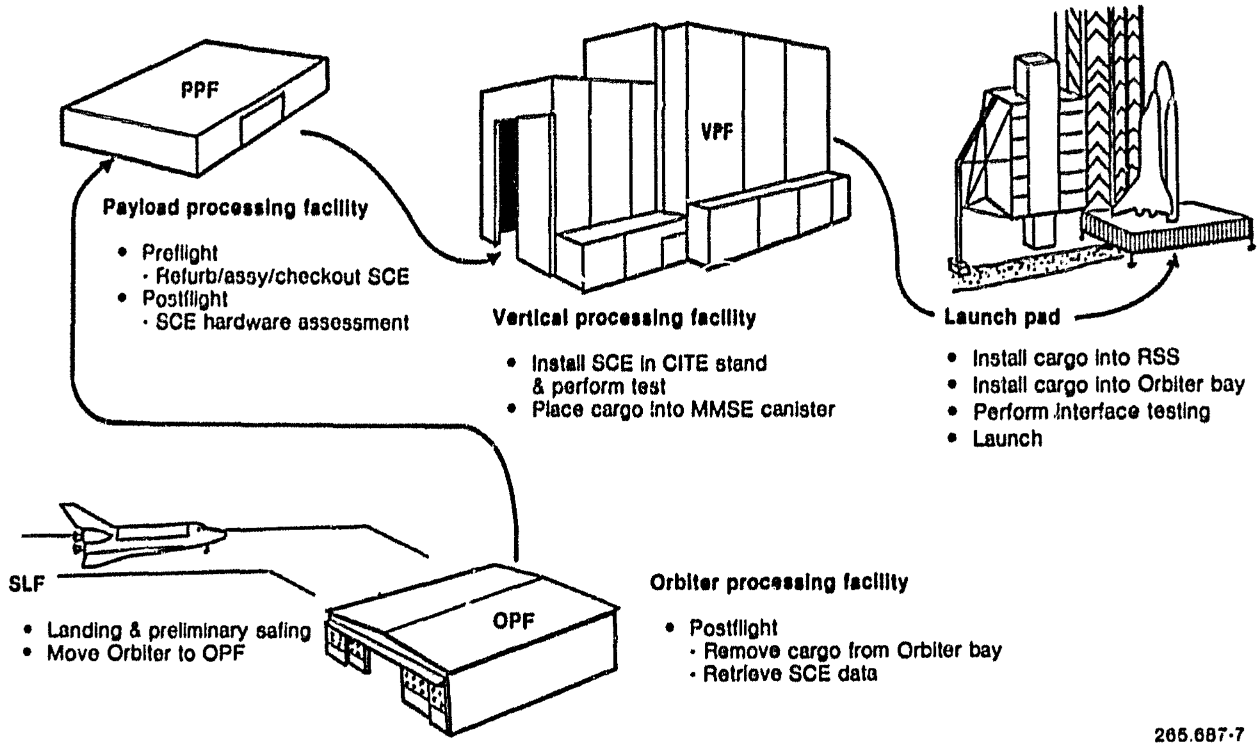

Figure 2-25. SCE Vertical Processing Operations

flight readiness. The SCE will then be transferred to either a Vertical or Horizontal Processing Facility where it will be integrated with other assigned coflight manifested payloads (into a complete cargo assembly) and processed for launch using conventional Shuttle Orbiter preflight procedures. Either the vertical or the horizontal processing mode may be used for the SCE, permitting flexibility in its selection for compatibility with other payloads.

The flight test operations sequence and timelines for the first day of the experiment are shown in Figure 2-26. The first day's activities include the series of controls and dynamics tests described in Figure 2-27.

The construction operations test sequence will be conducted on the second day of the experiment. This test sequence, illustrated in Figure 2-28, includes several assembly and installation tasks that require manual and EVA-assisted operations. The EVA tasks will be performed by the mission specialist and the commander. The payload specialist will continue to control and monitor the SCE from the aft flight deck control and display panel, while the pilot performs the RMS operations. The EVA will remain in effect until all equipment is fully stowed for reentry and landing.

Instrumentation requirements for the SCE are summarized in Table 2-5.

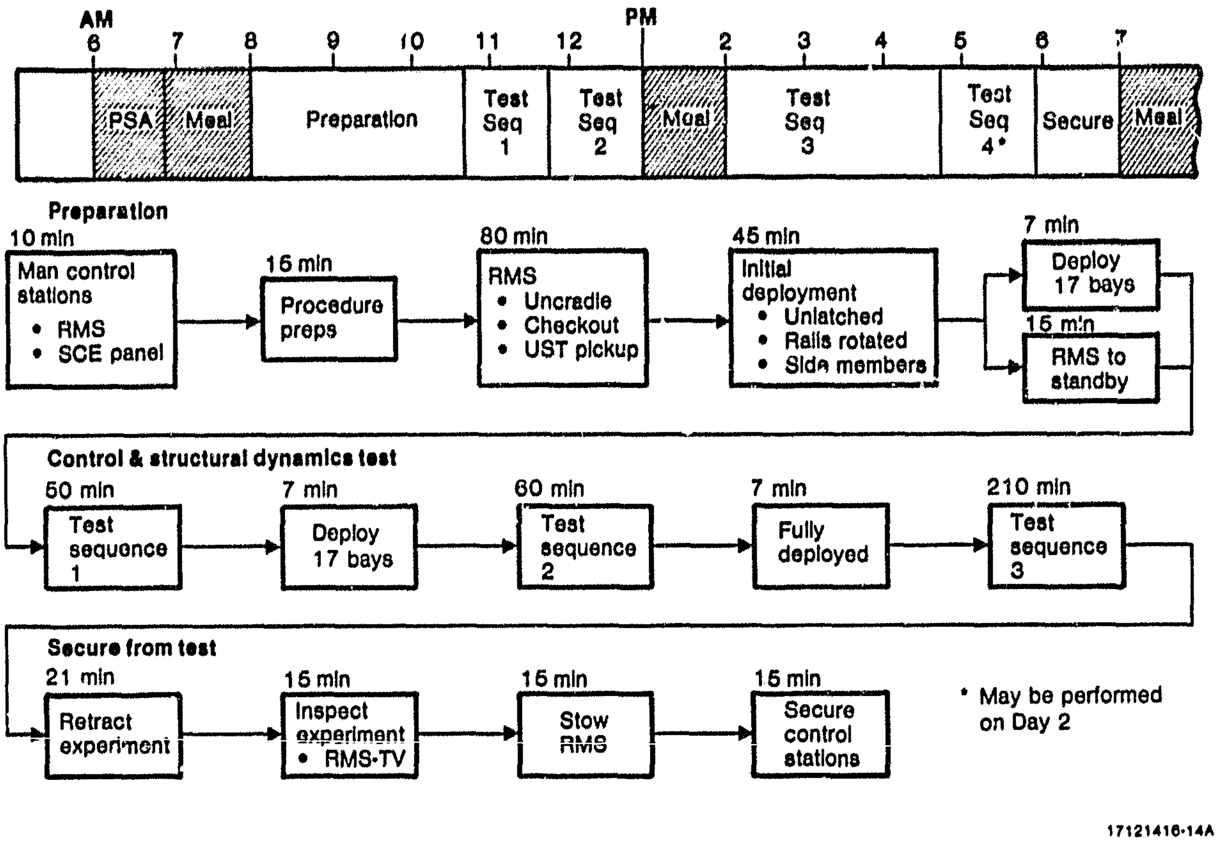

Figure 2-26. Flight Test Operations Sequence and Timelines for Day 1

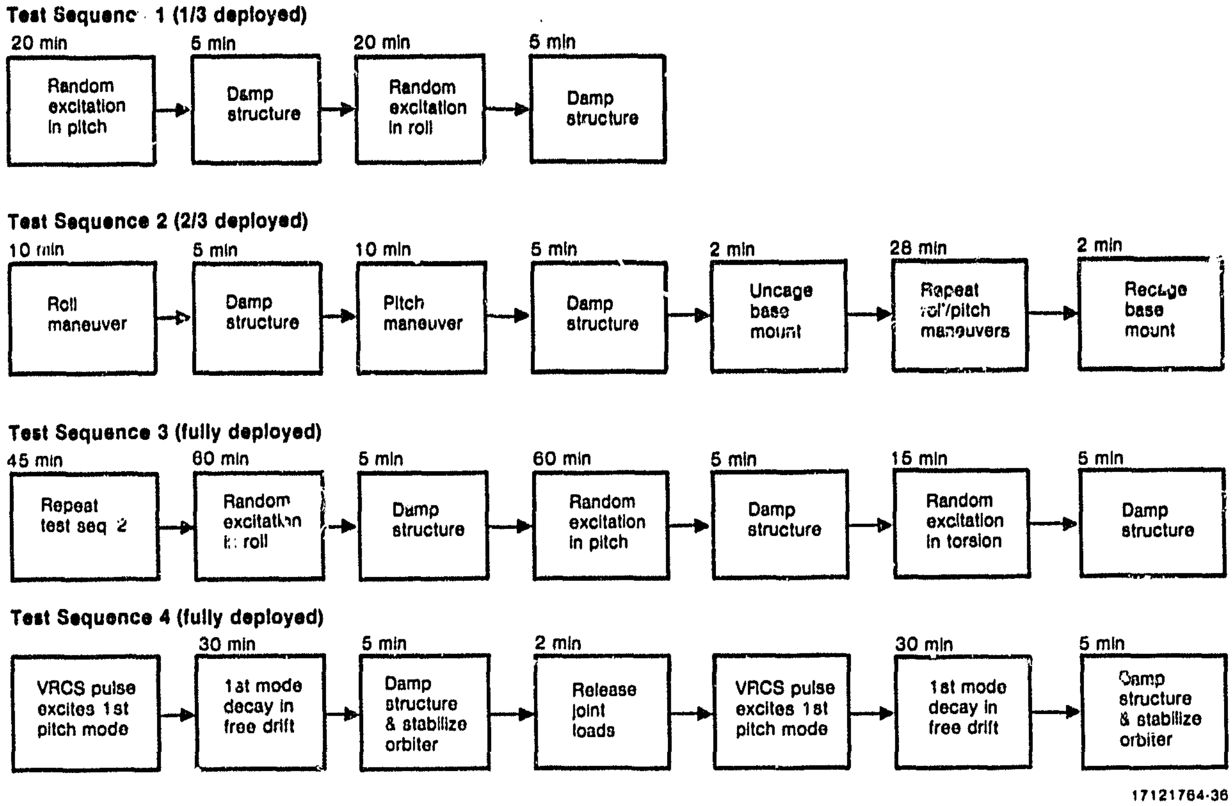

Figure 2-27. Structural Dynamics and Controls Flight Test Sequence

ORIGINAL PAGE IS OF POOR QUALITY

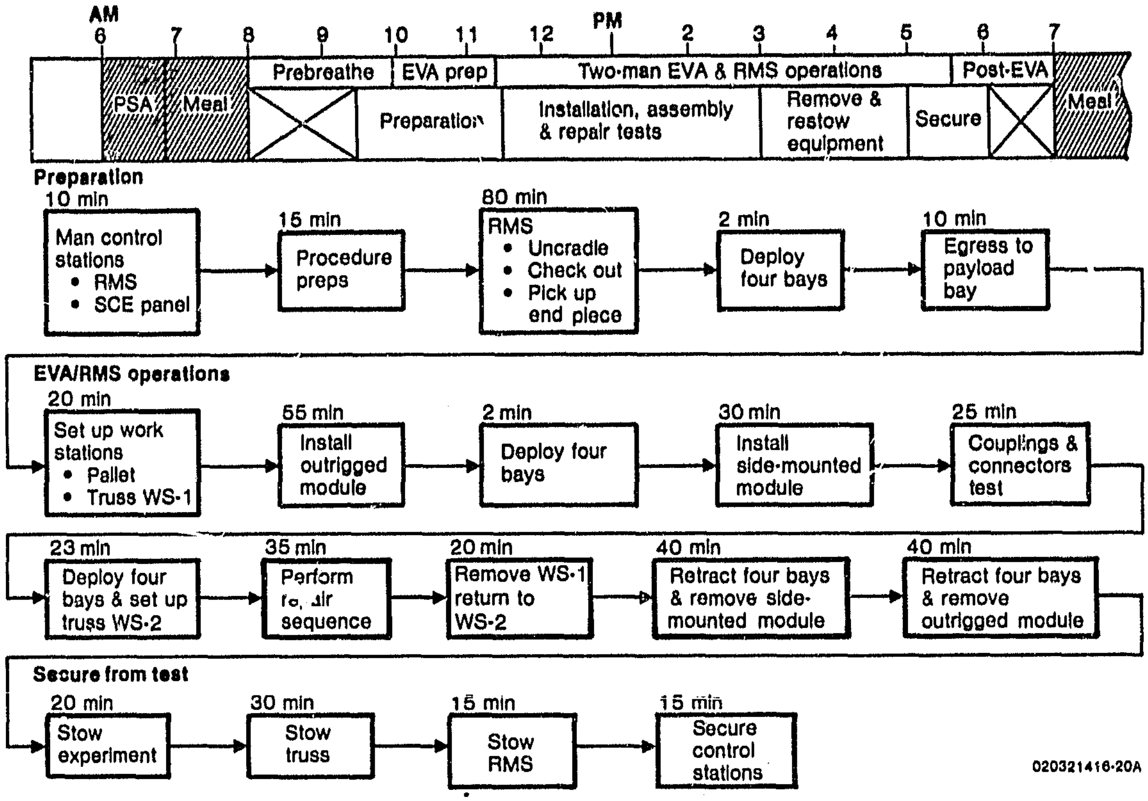

Figure 2-28. Construction Operations Test Sequence and Timelines for Day 2

Table 2-5. SCE Instrumentation Requirements

No.	Measurement	Type Sensor	Qty	Location
1	Tip motion rate	Rate gyro	6	1 each damper set
2	Mode shape & frequency	Servo-accelerometer Rate gyro P/E accelerometer	18 3 12	3 each at 6 truss stations 1 each at 3 truss stations 3 each at 4 truss stations
3	Z-axis acceleration	P/E accelerometer	1	Tip of truss
4	Tip deflection	Laser & detector array	1	Tip & base of truss
5	Carriage position	Rotary encoder	2	1 each deploy carriage
6	Motor temperatures	Thermocouple	10	2 each carriage 1 each damper set
7	Truss member load	Strain gauge	48	2 each longitudinal & diagonal, truss bay 33 & 50
8	Roll support loads	Strain gauge	4	1 each deployment rail Roll support lug
9	Pitch support loads	Load cell	2	1 each pitch brace
10	Trunion pin loads	Strain gauge	10	2 each pin
11	Trunion pin motions	Potentiometer	5	1 each pin

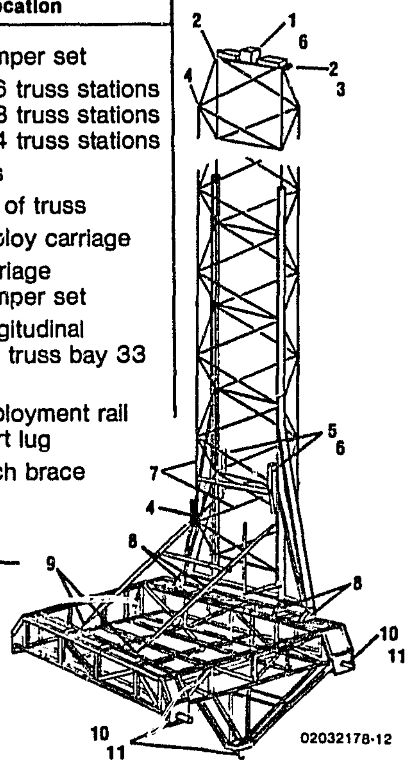

2.7 PROGRAMMATICS

2.7.1 PROGRAM DEVELOPMENT PLAN. Based on the overall program scope of this SCE and the desired milestones, two summary program development schedules have been established. The first schedule (Figure 2-29) represents a nominal development approach keyed to a flight in late CY86. The second schedule (Figure 2-30) is designed for a slower startup and a flight one year later in CY87.

In Option 1, the overall design and development schedule for this experiment provides a 42-month development program leading to the flight test in November 1986. The development period is preceded by a Phase A/B definition phase in 1981 and 1982.

In Option 2, the development period has been extended to 48 months and delayed to lessen the annual funding requirements and minimize the FY83 requirements but still provide for a flight in CY87. In this option, the program go-ahead is delayed to the last quarter of FY83, and the bulk of the contractor design and development testing, and fabrication and assembly is conducted in FY84 and FY85, respectively. Major testing is accomplished in FY86 and FY87, and the flight is scheduled in the last quarter of FY87.

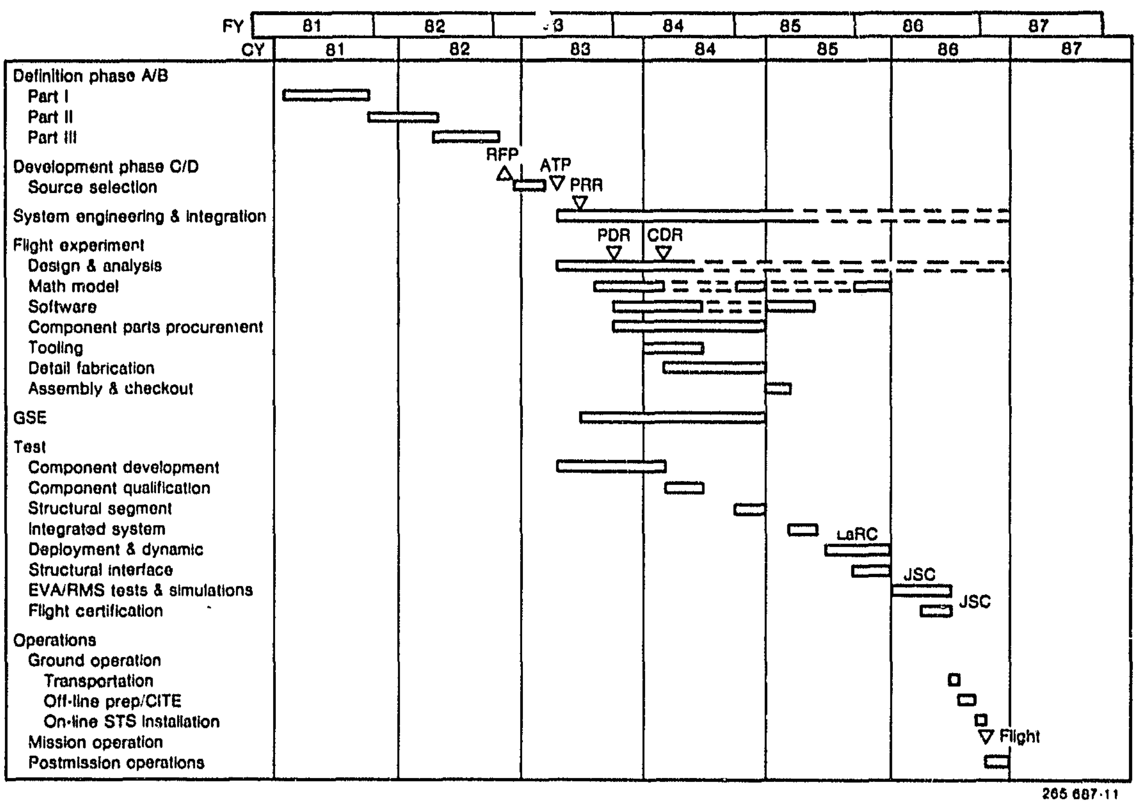

Figure 2-29. Preliminary SCE Program Development Schedule - Option 1

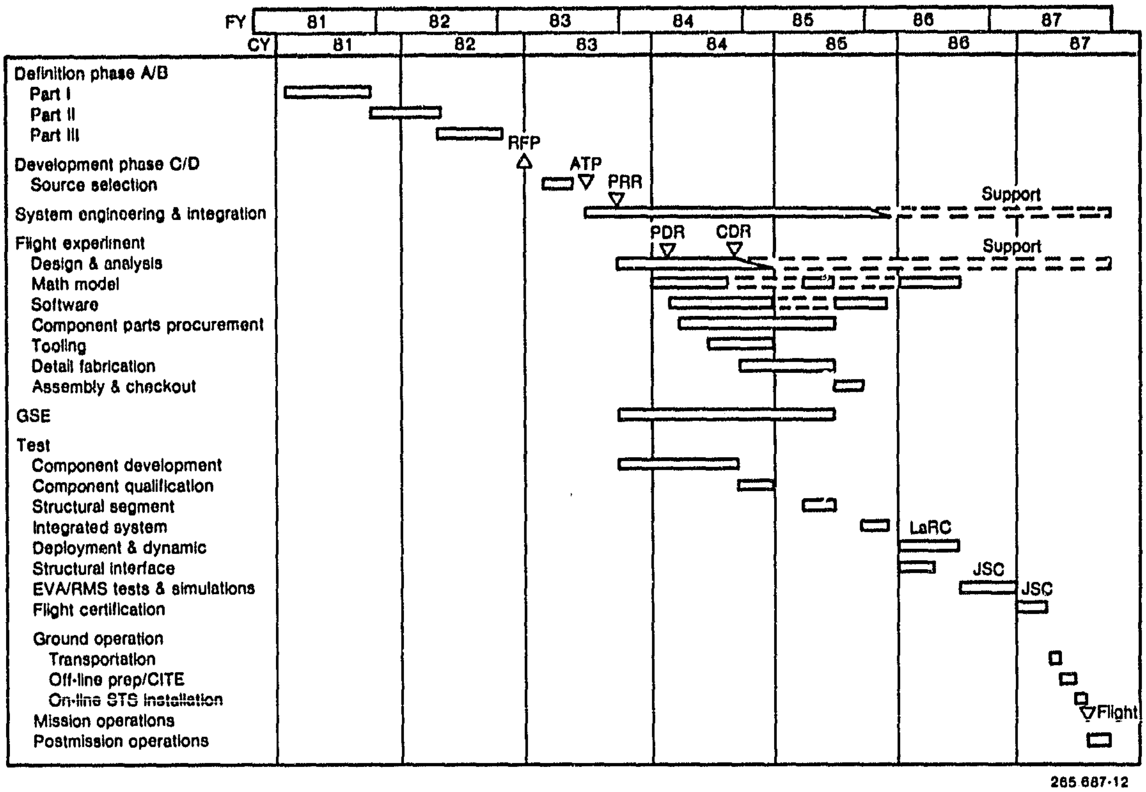

Figure 2-30. Preliminary SCE Program Development Schedule - Option 2

2.7.2 PROGRAM COST ESTIMATES. Using the updated information concerning the current SCE configuration generated in this phase of study, new cost estimates were made for the selected SCE as defined. The results of this analysis are presented in Figure 2-31. The total cost for the design, development, fabrication, and test of the SCE is approximately $12M. The experiment flight hardware fabrication accounts for about $5.3M and the remaining $6.9M is required for design and analysis, component development and test, system engineering, the system level test, program, and program management. It should be noted that all system level testing and integration is conducted using the flight experiment equipment that is subsequently refurbished for flight configuration.

The majority of the hardware design and development cost is required for structure and mechanisms including the truss, its deployment mechanism, and the supporting structure (FSE) for mounting the SCE in the Shuttle payload bay. The dynamic test equipment is considered as virtually all off-the-shelf equipment such as gyros and accelerometers and very little in the way of component development will be required. Only a nominal cost allowance is required for the RMS/EVA test equipment in that there are mass and form mockups only to establish the feasibility of attaching equipment to the truss beam.

Cost summary

Item	COST (1982 M$) Design & Development	Fabrication
Flight Hardware		
Structure	1.96	2.86
Dynamic Test Equipment	0.93	1.02
RMS/EVA Test Equipment	0.14	0.20
Flight Support Equipment	1.30	0.60
Assembly, Integration, and C/O	–	0.27
Software	0.20	–
System Engineering & Integration	0.77	–
System Test	0.78	0.13
GSE	0.16	–
Spares	0.27	–
Facilities	0	
Program Management	0.34	0.25
TOTAL	6.85	5.32
GRAND TOTAL	12.17	

COST GROUND RULES
- Costs are shown in constant 1982 dollars.
- Prime contractor fee is not included.
- Costs are for the design development and fabrication of a single, flyable experiment.
- All system testing required is accomplished using the flight article hardware.
- No mission operations or Shuttle user charges are included.
- The cost estimates presented are rough-order-of-magnitude costs for planning purposes only.

Annual funding (1982 $M)

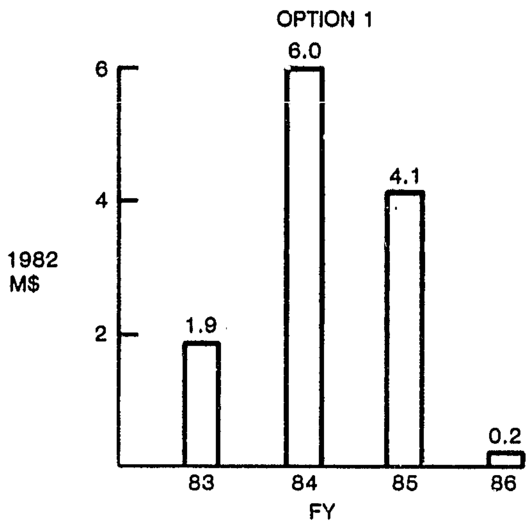

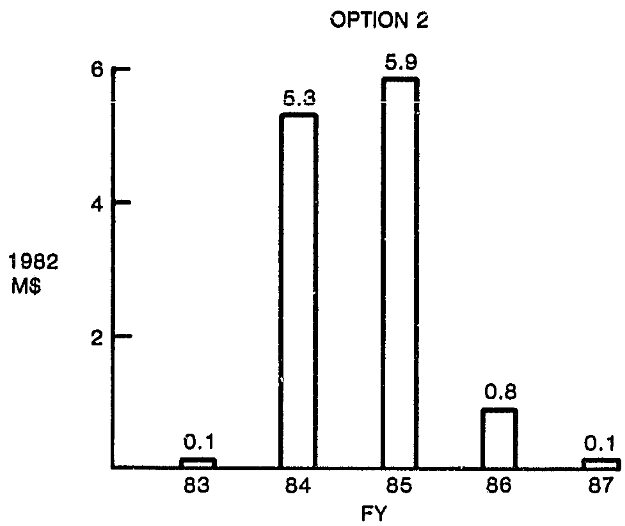

Figure 2-31. Preliminary Program Funding Requirements

Operations costs were not estimated at this time, but would consist of transportation (to KSC), ground operations for preparation for STS installation and postflight disposition, plus support activities during the flight. Annual funding requirements by fiscal year for development and flight article fabrication were generated by spreading individual cost elements in accordance with the program schedules. These annual funding requirements for the SCE are presented in Figure 2-31 and highlight the funding differences between the two schedule options.

SECTION 3
CONCLUSIONS AND RECOMMENDATIONS

3.1 CONCLUSIONS

- The basic requirements for a representative large space antenna feed mast can be satisfied with the tetrahedral deployable diamond truss.
- Use of torque wheels at the tip of the test structure offers an excellent solution for exciting the lower modes.
- Structural dynamic modeling accuracies are enhanced through component, subassembly, and partially deployed ground testing.
- A flexible base mount for the test structure allows the modal characteristics to be varied so that Orbiter DAP control capabilities can be challenged by approaching its control limits by degrees.
- Mission assignment is required to confirm the basic experiment envelope and Orbiter interfaces.
- Reduced modal frequencies of the test structure have been shown to provide a control challenge to the DAP.
- A 1986 flight is achievable if program start is initiated in early 1983.
- Total SCE program costs have escalated to over $10M as a result of the changes in requirements and greater detail of definition accomplished in Part II.

3.2 RECOMMENDATIONS

- Process request for preliminary mission assignment based on Part II results.
- Evaluate Part II preliminary design for cost reduction approaches.
- Further refine SCE preliminary design to incorporate cost reduction changes and mission assignment constraints.
- Perform preliminary design of EVA/RMS experiments.
- Perform preliminary design of potential add-on experiments such as plume effects measurements.
- Review CSDL DAP-structure interactions analysis data and refine modal excitation and DAP interactions amplitudes and loads.
- Perform dynamic analysis of partially deployed case.